DipSAR
Deep Image Prior for Sparse Sampled Near-Field SAR Millimeter-Wave Imaging

Assabumrungrat, Rawin; Kumchaiseemak, Nakorn; Wang, Jianping; Wang, Dingyang; Punpeng, Phoom; Fioranelli, Francesco; Wilaiprasitporn, Theerawit

DOI
10.1109/SENSORS56945.2023.10325198

Publication date
2023

Document Version
Final published version

Published in
Proceedings of the 2023 IEEE SENSORS

DipSAR: Deep Image Prior for Sparse Sampled Near-Field SAR Millimeter-Wave Imaging

Rawin Assabumrungrat[1,†], Nakorn Kumchaiseemak[2,3,†], Jianping Wang[3], Dingyang Wang[3],
Phoom Punpeng[4], Francesco Fioranelli[3,*], Theerawit Wilaiprasitporn[2,*]
[1]School of Engineering, Tohoku University, Japan
[2]School of Information Science and Technology, Vidyasirimedhi Institute of Science and Technology, Thailand
[3]MS3 Group, Department of Microelectronics, Delft University of Technology, The Netherlands
[4]Ruamrudee International School, Thailand
[†]Contributed equally
[*]Co-corresponding author

***Abstract*—We present a deep learning-based approach called *DipSAR* for reconstructing millimeter-wave synthetic aperture radar (SAR) images from sparse samples. The primary challenge lies in the requirement of a large training dataset for deep learning schemes. To overcome this issue, we employ the deep image prior (DIP) technique, which eliminates the need for a large dataset and instead utilizes only the sparse sample itself. Our proposed *DipSAR* model recovers missing samples from sparse data and reconstructs the SAR image using a conventional method. In this study, we utilize an existing SAR dataset and create fourteen different patterns to generate additional sparse samples by removing certain data points. We then evaluate the performance of DipSAR in comparison to the conventional method. The results show that DipSAR outperforms the conventional method in terms of the intersection over union (IoU) score.**

***Index Terms*—millimeter-wave, synthetic aperture radar, deep image prior, near-field imaging, sparse data**

I. Introduction

Nowadays, microwave imaging using near-field synthetic aperture radar (SAR) has become increasingly important in various scenarios, including the military and medical sectors. The unique ability of radio waves to penetrate and reflect off objects has led to numerous applications, such as concealed item detection [1] and small object detection [2]. However, constructing a near-field SAR imaging system faces significant challenges, including cost considerations and the need for a large number of transceiver antennas to achieve high-quality imaging details. Traditional methods address this by employing motion control to simulate ideal synthetic antenna arrays. Nevertheless, scanning a spatial area using this approach is time-consuming and has the risk of data loss during the scanning process, which adversely affects the image quality.

To address these challenges, recent developments have focused on techniques for SAR reconstruction with sparse data, such as the non-uniform fast Fourier transform range-migration algorithm [3]. Simultaneously, deep learning (DL) has gained significant attention in radar signal processing, particularly in SAR reconstruction, due to its promising results compared to state-of-the-art approaches. For instance, in [4], [5], a deep denoising technique is employed to achieve high-resolution SAR reconstruction, while another approach in [6], [7] utilizes a generative model to obtain highly detailed SAR images. However, a common drawback of most deep learning algorithms is their reliance on large amounts of training data to attain high-quality images.

In this paper, we introduce *DipSAR*, a deep learning framework designed for reconstructing sparsely sampled SAR images at mm-wave. *DipSAR* leverages the concept of deep image prior (DIP) [8] by modifying a non-trained generator to predict sparsely sampled data prior to reconstruction. In this approach, a fixed random noise is assumed as the input latent code, while the network parameters are optimized to represent the missing samples. The key concept is that the network structure itself acts as a robust regularizer. As a result, this technique eliminates the need for a large training dataset, as the network learns from the prior knowledge inherent in sparsely sampled data. The proposed method is evaluated with different types of sparsely sampled data, showing that it can outperform a conventional approach in terms of Intersection over Union (IoU) metric.

II. Data & Proposed Method

Our goal is to utilize DIP technique to recover the missing information from raw data and then reconstruct the SAR image using a conventional method [9]. First, we provide a comprehensive discussion on data preparation, focusing on experimentation with an existing dataset, which enables the performance assessment of our model (DipSAR) for this particular task. Then, our proposed method DipSAR is described with implementation details. The overview of the proposed approach is illustrated in Figure 1.

A. Data Preparation

The data utilized in our study are sourced from [10], which conducted spatial scanning across a 2-D plane $(x, y, z = 0)$. The data collection process involved transmitting and receiving antennas located in close proximity to each other, treated as a full duplex antenna transceiver positioned at the center. For

2023 IEEE SENSORS | 979-8-3503-0387-2/23/$31.00 ©2023 IEEE | DOI: 10.1109/SENSORS56945.2023.10325198

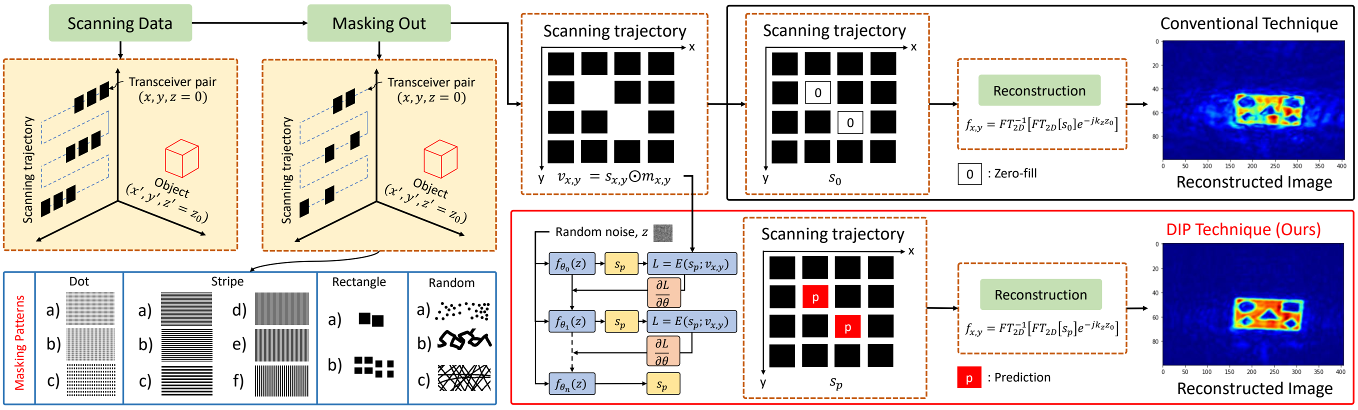

Fig. 1. Overview of the proposed approach and its verification. It consists of the scanning trajectories (yellow boxes), masking patterns (blue box), the conventional method (black box), and our proposed method (DipSAR) (red box).

a comprehensive understanding of the hardware configuration, please refer to the detailed explanation provided in [10].

Based on the measurement configuration, the receiving signal at the transceiver $s_{x,y}$ can be represented as the product of the reflectivity function $f_{x',y',z'}$ and the round trip phase. This relationship can be mathematically defined as:

$$s_{x,y} = \iint f_{x',y',z_0} \cdot e^{-j2k\sqrt{(x-x')^2+(y-y')^2+z_0{}^2}} dx'dy', \quad (1)$$

where k is the wavenumber. The fundamental concept behind reconstructing a 2-D SAR image involves the recovery of the reflectivity function from Equation (1).

A well-known and widely recognized algorithm involves leveraging the Fourier-transform to reformulate Equation (1), enabling the removal of the primed and unprimed coordinate system, as they coincide. This yields the following reconstruction equation below:

$$f_{x,y} = FT_{2D}^{-1}[FT_{2D}[s_{x,y}] \cdot e^{-jk_z z_0}] \quad (2)$$

and

$$k_z = \sqrt{4k^2 - k_x^2 - k_y^2} \quad (3)$$

where, k_x, k_y, and k_z are the wavenumber corresponding to each Cartesian coordinate, decomposed from k based on electromagnetic dispersion relation.

In our experiment, we simulate the sparsely sampled data $v_{x,y}$ by generating a binary masking pattern $m_{x,y} \in \mathbb{Z}_2$. This pattern is utilized to selectively remove portions of the receiving signal, as defined by the following relation:

$$v_{x,y} = s_{x,y} \odot m_{x,y} \quad (4)$$

where $\odot$ is Hadamard's product. To generate diverse types of sparse data, we have designed a set of fourteen masking patterns. These patterns vary in terms of shape and size, including three different sizes of dots (2x2, 3x3, and 5x5 samples), three different line heights for horizontal stripes (2, 3, and 5 samples), three different line widths for vertical stripes (2, 3, and 5 samples), two large rectangles, four small rectangles, random dots, random drawings, and random lines, as illustrated in Figure 1 (blue box).

B. *DipSAR*

In our proposed approach, we employ DIP networks to recover the receiving signal from the sparsely sampled signal. DipSAR acts as a generative network approach, generating missing samples instead of relying on a regularization term for reconstruction. This is achieved by incorporating DIP as the reparameterization function $s_{x,y} = f_\theta(z)$, where f_θ is the deep generative network with weights θ, and z is a fixed random noise. As a result, the optimization function for DipSAR can be expressed as:

$$\hat{\theta} = \arg\min_{\theta} ||f_\theta(z) - v_{x,y}||^2, \quad s_p = f_{\hat{\theta}}(z) \quad (5)$$

where s_p is the predicted signal and $\hat{\theta}$ is the paremeters to be minimized that can be optimized using Adam optimizer.

Next, we employ the conventional method (equation 2) to reconstruct the SAR image based on the predicted signal. The algorithm for image reconstruction is outlined in Algorithm 1.

Algorithm 1 DipSAR: SAR image reconstruction using DIP

Pre-processing

1: Collect uniformly complex FMCW samples from transceiver scanning over a 2-D planar aperture
2: Select z_0 to focus on the object, resulting a receiving signal $s_{x,y}$
3: Mask out samples $v_{x,y} = s_{x,y} \odot m_{x,y}$

Training

1: Input: fixed random noise z, sparse sampled signal $v_{x,y}$
2: Output: predicted signal s_p
3: **for** number of training iterations **do**
4: $\quad s_p = f_\theta(z)$
5: $\quad$ Compute $L = ||s_p \odot m_{x,y} - v_{x,y}||^2$
6: $\quad$ Update weight θ using Adam optimizer
7: **end for**

Post-processing

1: Reconstruct image using: $f_{x,y} = FT_{2D}^{-1}[FT_{2D}[s_p] \cdot e^{-jk_z z_0}]$

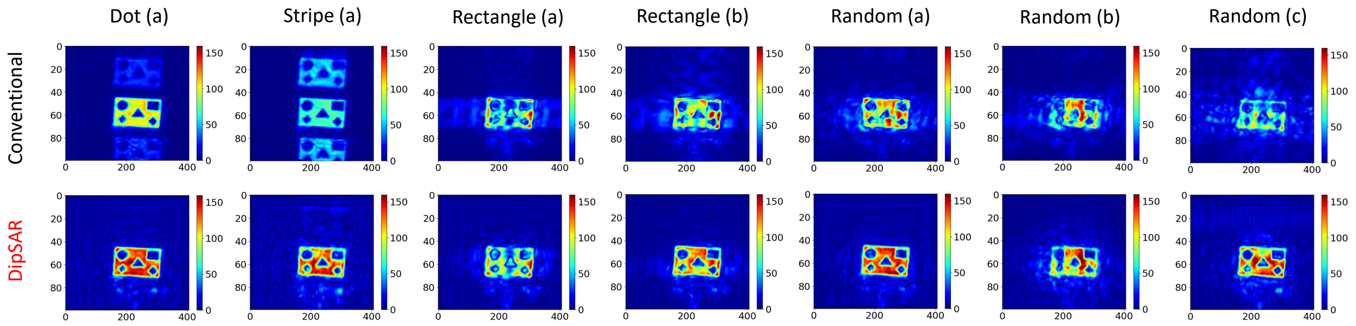

Fig. 2. Qualitative comparison of the conventional method and DipSAR. Our DipSAR predictions are closer to the ground truth [10] with fewest outliers.

TABLE I
RECONSTRUCTION RESULTS VIA IOU SCORES AT 3 DIFFERENT THRESHOLDS.

	IoU ↑					
	$Thres_{40}$		$Thres_{60}$		$Thres_{80}$	
Patterns \ Methods	Conv.	DIP	Conv.	DIP	Conv.	DIP
Average Dot	0.928	**0.939**	0.898	**0.946**	0.853	**0.934**
Average Stripe	0.615	**0.922**	0.691	**0.931**	0.238	**0.901**
Average Rectangle	0.705	**0.796**	0.649	**0.758**	0.463	**0.671**
Average Random	0.714	**0.891**	0.658	**0.875**	0.486	**0.838**

C. Implementation Details

For DipSAR, we adopt a UNet architecture [11] with the input $z \in \mathbb{R}^{C\times W\times H}$ and the output $f_\theta(z) \in \mathbb{C}^{W\times H} \in \mathbb{R}^{2\times W\times H}$ having a similar number of spatial samples, where the parameter C is set to 32. The learning rate is set to 1×10^{-2}. Due to the limited number of samples, we are unable to employ the early stopping scheme, which typically relies on a large validation set to prevent network overfitting as in the original DIP approach. Instead, we optimize the iteration count to 3000, based on the best average performance observed during each training. Training DipSAR typically takes approximately 5 minutes on a single NVIDIA GeForce RTX 2080Ti.

III. RESULTS AND DISCUSSION

In this section, we evaluate the performance of our method using the Intersection over Union (IoU) metric, which provides an indication of how well our reconstruction method aligns with the original, ground-truth image. In Section III-A, we provide a comprehensive overview of the conventional method, highlighting its details and comparing it to our method for reconstruction tasks. Following that, Section III-B discusses of the limitations of our work.

A. Comparison to the conventional method

In this experiment, we conduct a comparative analysis between DipSAR and the conventional method in terms of their reconstruction performance, which is measured by the IoU score of the SAR image. The conventional method [12] yields the SAR image by filling zeros in the sparsely sampled signal $v_{x,y}$, resulting in s_0. Then, equation (2) is computed to obtain the SAR image.

The IoU metric is commonly utilized to quantify the overlapping region between the predicted and ground-truth images. However, as discussed in Section II, our SAR images represent the reflectivity function, which consists of continuous values. Therefore, directly estimating the IoU from the original SAR image is not feasible. To address this, we convert the SAR image into a binary image by applying a constant threshold value. By using this threshold, reflectivity values exceeding it are set to one, while the remaining values are set to zero. In our study, we propose three different constant thresholds to comprehensively cover various signal strengths. The results, both quantitative and qualitative, are presented in Table I and Figure 2, respectively.

B. Limitation

This initial study showcases the strong performance of DipSAR in reconstructing sparsely sampled SAR data. However, there are certain limitations to consider. It is crucial to preserve rich information, particularly in the object area, as the model relies on this information to capture prior knowledge of the image. In cases where such information is removed, such as in rectangle (a) and random (b) masking, the performance is less good. Additionally, our investigation is limited to a specific set of masking patterns and data, leaving the generalization ability of the model unexplored in this study.

IV. CONCLUSION

We have introduced a novel approach called *DipSAR*, which utilizes the DIP technique for sparsely sampled SAR image reconstruction. Our model takes fixed random noise as input and predicts missing samples from the sparsely sampled data. A conventional method is then employed to reconstruct the SAR image. The use of DIP eliminates the need for supervised data, allowing for its application in real-world scenarios where certain scanning trajectories may be missing. Furthermore, our study includes various types of masking to simulate diverse possibilities encountered in real-world scenarios. The experimental results demonstrate that DipSAR outperforms the conventional method in terms of average IoU scores.

REFERENCES

[1] X. Zhuge and A. G. Yarovoy, “A sparse aperture mimo-sar-based uwb imaging system for concealed weapon detection,” *IEEE Transactions on Geoscience and Remote Sensing*, vol. 49, no. 1, pp. 509–518, 2011.

[2] N. Kumchaiseemak, I. Chatnuntawech, S. Teerapittayanon, P. Kotchapansompote, T. Kaewlee, M. Piriyajitakonkij, T. Wilaiprasitporn, and S. Suwajanakorn, “Toward ant-sized moving object localization using deep learning in fmcw radar: A pilot study,” *IEEE Transactions on Geoscience and Remote Sensing*, vol. 60, pp. 1–10, 2022.

[3] J. Wang, P. Aubry, and A. Yarovoy, “3-d short-range imaging with irregular mimo arrays using nufft-based range migration algorithm,” *IEEE Transactions on Geoscience and Remote Sensing*, vol. 58, no. 7, pp. 4730–4742, 2020.

[4] M. B. Alver, A. Saleem, and M. Çetin, “Plug-and-play synthetic aperture radar image formation using deep priors,” *IEEE Transactions on Computational Imaging*, vol. 7, pp. 43–57, 2021.

[5] H. Lin, Y. Zhuang, Y. Huang, and X. Ding, “Self-supervised sar despeckling powered by implicit deep denoiser prior,” *IEEE Geoscience and Remote Sensing Letters*, vol. 19, pp. 1–5, 2022.

[6] K. Wang, G. Zhang, Y. Leng, and H. Leung, “Synthetic aperture radar image generation with deep generative models,” *IEEE Geoscience and Remote Sensing Letters*, vol. 16, no. 6, pp. 912–916, 2019.

[7] H. Huang, F. Zhang, Y. Zhou, Q. Yin, and W. Hu, “High resolution sar image synthesis with hierarchical generative adversarial networks,” in *IGARSS 2019 - 2019 IEEE International Geoscience and Remote Sensing Symposium*, 2019, pp. 2782–2785.

[8] D. Ulyanov, A. Vedaldi, and V. Lempitsky, “Deep image prior,” *International Journal of Computer Vision*, vol. 128, no. 7, pp. 1867–1888, Mar. 2020. [Online]. Available: https://doi.org/10.1007/s11263-020-01303-4

[9] D. Sheen, D. McMakin, and T. Hall, “Three-dimensional millimeter-wave imaging for concealed weapon detection,” *IEEE Transactions on Microwave Theory and Techniques*, vol. 49, no. 9, pp. 1581–1592, 2001.

[10] M. E. Yanik and M. Torlak, “Near-field 2-d sar imaging by millimeter-wave radar for concealed item detection,” *2019 IEEE Radio and Wireless Symposium (RWS)*, pp. 1–4, 2019.

[11] O. Ronneberger, P. Fischer, and T. Brox, “U-net: Convolutional networks for biomedical image segmentation,” in *Medical Image Computing and Computer-Assisted Intervention – MICCAI 2015*, N. Navab, J. Hornegger, W. M. Wells, and A. F. Frangi, Eds. Cham: Springer International Publishing, 2015, pp. 234–241.

[12] S. Kharkovsky and R. Zoughi, “Microwave and millimeter wave nondestructive testing and evaluation - overview and recent advances,” *IEEE Instrumentation Measurement Magazine*, vol. 10, no. 2, pp. 26–38, 2007.